Supplementary Material

Methods

General

Single cell and multiunit signals were recorded by a multichannel recording system (Plexon Inc, Texas) from 96 paralyne coated tungsten or platinum/iridium electrodes (impedance ≈ 300 kΩ) (Microprobe Inc. Maryland) implanted in the medial intraparietal area (MIP), a subdivision of the parietal reach region (PRR), and area 5 (*1*) of three rhesus monkeys trained to perform a memory reach task. One monkey (monkey S) also had 64 electrodes implanted in the dorsal premotor area (PMd) in a separate surgery. Each session consisted of a *reach segment* and a *brain control segment*. Trials in both segments were initiated in the same way: after the monkeys acquired a central red fixation point with the eyes and touched a central green target, a peripheral cue was flashed indicating the location of one out of four, five, six, or eight reach targets (Figure 1a) (cue epoch). Reach targets were uniformly distributed around the central fixation point. As soon as the fixation point and central green target were acquired, hand and eye movements were restricted by a real time behavioural controller (LabVIEW, National Instruments). Eye position was monitored using a scleral search coil (CNC Engineering, monkeys S and O), or an infrared reflection system (ISCAN, monkey C) while hand position was monitored using an acoustic touch screen (ELO Touch). In order to successfully complete a trial, the monkeys were not allowed to move their eyes. In addition, the reaching hand had to be in contact with the centrally located green target at all times except after the GO signal which appeared during the reach segment of the session. After the offset of the cue, a delay of 1.5 ± 0.3 seconds ensued. During the reach segment, the green central target was extinguished after the memory period

indicating to the animal to reach to the remembered target location (motor epoch). After reaching to the location of the extinguished cue, the monkeys had to maintain contact with the screen for 350ms. If successful, the cue was illuminated and the monkeys had to maintain contact with the visible target for an additional 300ms before they were rewarded. Any break in eye fixation during the trial aborted it.

In the brain control trials the intended reach location was decoded from a 900 ms interval of the delay period starting 200 ms after cue offset. Unless otherwise noted, all brain control analysis and tuning curves of cells presented in this study are based on this 900 ms interval. If the correct position was decoded, the cue location was illuminated with a larger cue and the monkeys received a reward. The monkeys were not allowed to reach or break fixation until after the reward had been delivered. No feedback was given to the monkeys when the wrong target location was decoded. Instead, the green central target was extinguished indicating to the monkeys to initiate a reach. Therefore the monkeys had to continue with a failed decode trial as if it was a reach trial. The adaptive database was not updated after the failed decode trials (see below).

Variable Reward

Only a single aspect of the reward (magnitude, probability or type) was varied during a given session. The size of the cue indicated the magnitude or type of reward, or the probability of obtaining a reward. In order to control for the effects of cue size on the firing rate, the association between cue size and reward was varied on different sessions. The mapping of cue size to reward condition had no effect on the representation of expected value. The magnitude of the reward was 0.05ml and 0.12 ml for low and high volume respectively. When probability was varied, a constant volume reward (0.12 ml)

was delivered either 40% or 80% of the time upon successful completion of the trial. Hence, the monkeys were not rewarded on all trials but had to complete all the trials presented. When reward size or type was varied, reward probability was fixed at 100%. Reward type (orange juice vs. water) was delivered from two sipper tubes that were calibrated to dispense equal volumes of liquid. The sipper tubes were placed near the monkey's mouth with the location of the tube altered on different days. No effect of juice tube placement on the firing rate was found.

Database

During the reach trials, the activity of all the cells was recorded and a database containing the firing rates was constructed. Once enough trials were collected (30 reaches for each target location except the PMd recordings which used 20 reaches per target location), the brain control segment of the task was initiated. The goal of this segment was to have the monkeys position a cursor on the screen with their thoughts. A selection of single and multiunit activity was then chosen from the database predicated on their tuning properties assessed using an ANOVA on the spiking activity during a 900 ms interval of the memory period beginning 200 ms after cue offset. Many more neurons than those chosen were recorded from the arrays. For example, many cells exhibited strong visual and motor related activity. This activity was also tuned and can easily be used to decode target location with a high success rate (Figure S1). However, our goal is to decode intentions represented by cognitive signals and not responses directly elicited by stimuli or neural activity associated with overt movements. Therefore, only those neurons that showed clear tuning in the memory period as assessed by the ANOVA were chosen for the decode (monkey S (parietal): range = [5, 13], median = 6; monkey C:

range = [4, 48] median = 6.5; monkey O: range = [6, 10], median = 7.5; monkey S (premotor): 3 sessions using 8, 15 and 16 neurons. median = 15). (For the first 5 sessions of monkey C, we did not utilize the results of the ANOVA but instead used 48 channels for the decode).

Decode Algorithm

The movement intention that was encoded by the neural activity in the memory period for each trial in the brain control task was then decoded using a Bayesian algorithm on a family of Haar wavelet coefficients (*2*). Bayes rule is defined by $P(s \mid r) = \frac{P(r \mid s)P(s)}{P(r)}$ where r is the response and s is the target direction. $P(s|r)$ was calculated for all directions and the direction decoded taken to be the maximum of all $P(s|r)$. 100 wavelet coefficients were calculated by projecting the spike train recorded during 900 ms of the memory period onto a family of Haar wavelet functions. In this way, temporal features in the spike train that cannot be described by the number of spikes in the memory period (equivalent to firing rate) were exploited (*2*). Haar wavelets are defined by (*3*):

$$\Psi(t) = \begin{cases} 1 & if\ 0 \le t \le \frac{1}{2} \\ -1 & if\ \frac{1}{2} \le t < 1 \\ 0 & otherwise \end{cases}$$

where dilations and translations of Ψ generate the orthonormal basis:

$$\Psi_{j,n}(t) = \frac{1}{\sqrt{2^j}} \Psi\left(\frac{t - 2^j n}{2^j} \right)$$

where j and n are integers that represent the frequency content of the wavelet. Note that the zeroth wavelet coefficient ($j,n,t = 0$) is simply the number of spikes in the 900 ms

portion of the memory epoch used in the decode since the wavelet being projected onto it is the step function. The Haar wavelets improved the Bayesian decode by taking advantage of the temporal features of the spike train in the memory period. Although we calculated a large number of coefficients, only a few (usually less than 5) had relevant information. The optimal coefficients can be calculated by applying sorting algorithms to the coefficients based on information theory (2).

Offline decode on 10 sessions using a Bayesian algorithm with wavelets yielded a performance that was on average 6.6 ± 2.9 % better than offline decode that did not use the wavelets (range = [-0.4 9.1]). The number of spikes in the memory period (zeroth wavelet coefficient) yielded the greatest amount of information about the intended goal. The first wavelet coefficient also yielded tuned information useful for decode. The significance of this coefficient implies that the delay period had a different rate at the first and second half of the memory period that was useful for decoding.

The brain control session shown in the left panel of Figure 1D is based on a database composed of 20 reaches / direction. However, we used 50 reaches / direction to build the database for the offline decode. Not only did the decode performance improve using a greater number of neurons, but it also improved by using a greater number of trials in the database (87 % for 8 targets using all 16 neurons; Figure 1D right panel). However, for the 4 target decode, which is the main experimental condition used in this study, 30 reaches per direction was optimal as indicated by offline simulations.

Off-line decode results suggest that we can also improve the performance using larger training sets with a Fisher linear discriminant (FLD) algorithm. Using data obtained during brain control trials to run offline decodes, FLD improved the decode by 8.7 ± 6.2 % (mean ± standard deviation). However, we decided not to use this algorithm

on-line since the number of trials needed in the training set that would yield a decode performance better than the Bayesian algorithm approached 100 reaches / direction. This would substantially reduce the number of decode trials and was not even possible for some 6 target sessions. The use of a database with a small number of trials is more advantageous for neural prosthetics since patients do not need to be burdened with prolonged training sessions.

Adaptive vs. Frozen databases

Most sessions were run using the adaptive database but, on occasion, the frozen database was used (189 adaptive, 10 frozen). The adaptive database was simply a fixed (30 trials per direction) database moving in time. The database was continuously updated with new successful trials while old trials were removed using a first-in-first-out rule. This way, the database always contained the latest 30 successful trials per direction. The frozen database was composed of the trials collected during the reach segment of the session. Thereafter, the database was not updated but was frozen in time. Offline analysis indicated that no advantage was gained by using either approach (Figure S2). Mean success rate for monkey S for all sessions achieved using the adaptive decode (mean ± standard deviation) is 43.3 ± 11.1 % while the success rate using the frozen database is 42.1 ± 11.7 %. The two distributions are not statistically different.

Mutual Information

Mutual information is a useful measure as it quantifies the degree of tuning of a neuron as opposed to a statistical p – value which merely provides a probability of

whether a neuron is tuned or not (*4, 5*). The information carried by neurons was calculated using (*6*):

$$I(r,s) = \sum_{r,s} P(r,s) \log \frac{P(r,s)}{P(r)P(s)}$$

where *s* is the target direction and *r* is the response and the *log* is base 2. For brain control and reach trials, the mutual information was calculated on an equal number of trials. The joint distribution *P(r,s)* was estimated using a 2-D histogram between the stimulus and the response. The number of directions in a particular session dictated the number of stimulus bins in the histogram. Eight bins were used for the response which places the histogram outside the sparse region (*5*). The marginal distribution of the 2-D histogram was then used as an estimate of the probabilities *P(r)* and *P(s)*.

Learning statistics.

Figure 2B in the main text shows the mean mutual information from reach and brain control for each of 68 consecutive sessions for monkey S. During the first 20 sessions, the information about target location is high during the reach segment (when the database was being built) and much lower during the brain control segment for the same cells. The mean of the difference in the mutual information between the reach and the brain control segments for the first 20 sessions was 0.11 ± .002 bits (mean ± standard error) and was significantly different from zero (t-test, $P < 0.01$). The difference for the last 20 sessions was 0.028 ± .004 bits, also significantly different from zero ($P < 0.01$). However, the difference during the first 20 sessions is significantly greater than the difference from last 20 sessions ($P < 0.01$). Therefore, the information carried by cells recorded during the same session increased more during the brain control segment than

during the reach segment over the course of 68 sessions. This effect can also be seen by considering the rate of information increase within the reach and brain control segments. The regression slope for the mutual information during the reach segment was 0.0023 ± 0.0003 bits/session while the slope of the best fit regression line for the mutual information during brain control was 0.0031 ± 0.0003 bits/session. Both these slopes are significantly different from zero (t-test, $P < 0.01$). However, the rate of increase of the information during the brain control segments is greater than the rate of increase during the reach sessions (regression of the difference between reach trials and brain control trials is -0.0018 ± 0.0004 bits/session which is significantly less than zero $P < 0.01$). The same effect was shown by monkey C with less difference (regression of the difference between reach trials and brain control trials is -0.0008 ± 0.0003 bits/session which is significantly less than zero, $P < 0.01$).

The slope of the performance as a function of session number is 0.48 ± 0.25 percentage points / session for the last 10 sessions which is statistically greater than 0 ($p<0.02$) (Figure 2A). This positive slope implies that the performance may have continued to increase if more sessions were performed.

Electromyography

Percutaneous EMGs were recorded from the anterior deltoid (Figure S3), posterior deltoid, the rhombus and the lower trapezius of monkey C over 5 separate sessions during reach trials. EMG's were low-pass filtered (cutoff 1000hz), sampled at 2500 Hz and rectified before alignment. If the neural activity of the memory period was related to the direct activation of muscles, then increased EMG should be observed when the monkey is planning a movement in a muscle's preferred direction. Likewise, if the

increased direction tuning during preferred rewards is related to muscle activation then there should be an increase in EMG direction tuning for the preferred rewards. For all individual muscles tested, there was no statistically significant EMG directional tuning in the delay period during brain control trials for either the low or high reward condition. For the anterior deltoid example shown in Figure S3, the EMGs during the memory period increased by up to 4% when the preferred reward was indicated but this increase was not directionally tuned. Changing the reward had no effect on the activity of the rhombus, posterior deltoid or the trapezius. Thus, the directionally tuned increase in neural activity recorded in the high reward condition during the memory period was not associated with a significant directionally tuned increase in limb EMG.

Reaction Time

Reward manipulation also affected behavioral performance. The reaction time from the GO signal to the beginning of the movement of all trials during the reach segment of sessions using variable rewards was calculated. The expectation of preferred reward decreased the mean reach reaction time from 320 ± 1.51 ms to 309 ± 1.35 ms (mean ± standard error) (Figure S4). Reaction time is significantly smaller for the preferred reward condition ($P < 0.01$). This enhanced motor performance is consistent with increased motivation.

Expected Value Decode

We can decode the expected value of the reward. Figure S5A depicts an off-line decode of expected value of reward type using a frozen database for one brain control session. This binary decode was run independent of reach direction. For the same cells

used to decode direction, we can correctly identify whether the reward on the current trial is orange juice or water over 85% of the time (Figure S5A). Repeating this analysis over all the sessions for monkeys S and C and O, we can decode the expected value with an overall mean of 80.4 ± 8.6 %. For reach trials, decode performance was 74.5 ± 5.2 %. For brain control trials, decode performance was 84.7 ± 8.5 % (mean ± standard deviation) (Figure S5B).

Decode Interval Length

Offline decode on brain control trials indicated that memory period intervals as low as 100 ms can yield decode rates that are significantly greater than chance (Figure S6). There is however a steady increase in the performance as the interval size increased. No conclusion can be made on whether asymptotic behavior was reached since performance continued to increase as the limit of the memory period was reached. Time intervals extracted from the beginning of the memory period yielded better feedback performance than the same sized intervals from latter portions of the memory period (based on offline analysis on 5 sessions with high performance from monkey S. Brain control performance for 100 ms obtained from the beginning of the memory period was 51.2 ± 4.7 % while 100 ms obtained from the end of the memory period yielded a performance of 38.9 ± 7.2 % (chance 25%)).

Figure S1

Cumulative percent of correctly decoded trials using 700 ms of the motor burst (-100 ms to 600 ms after the GO signal in reach trials) of 4 parietal neurons during reach trials for 1 session.

Figure S2

Offline decode results performed with an adaptive (red) and frozen (black) database for all the sessions in consecutive order for monkey S. No statistical difference exists between the 2 populations.

Figure S3.

Percutaneous EMG recorded from the anterior deltoid of monkey C during reach trials. Black: high reward. Red: small reward. Plots are aligned to the onset of the cue. Reach directions are indicated on the plot. EMGs were smoothed with a moving window of 10 trials.

Figure S4.

Reach reaction time for preferred (n = 6671 reaches) and nonpreferred (n = 7180 reaches) conditions for monkeys S and C. Bars are SE.

Figure S5.

A) Decode result of expected value from a single brain control session and B) all the sessions where expected value of reward was manipulated. Error bars are standard deviation obtained by crossvalidation (leaving 30 trials out per

iteration). Sessions are not in consecutive order. The first 36 sessions are reach sessions (red) and the last 44 sessions are brain control sessions (black). Dashed line is chance.

Figure S6.

Offline decode on 16 sessions from monkey S using various time interval lengths of the memory period. Note that the time on the x-axis is not continuous but represents the length of the memory period that yielded the corresponding feedback performance. All intervals shown start 200 ms after the offset of the cue and last for the duration indicated on the x-axis. For example, the corresponding y -value at the interval marked 0.2 seconds corresponds to 200ms of the memory period starting 200 ms after the onset of the memory period (201-400ms of the memory period).

Figure S1

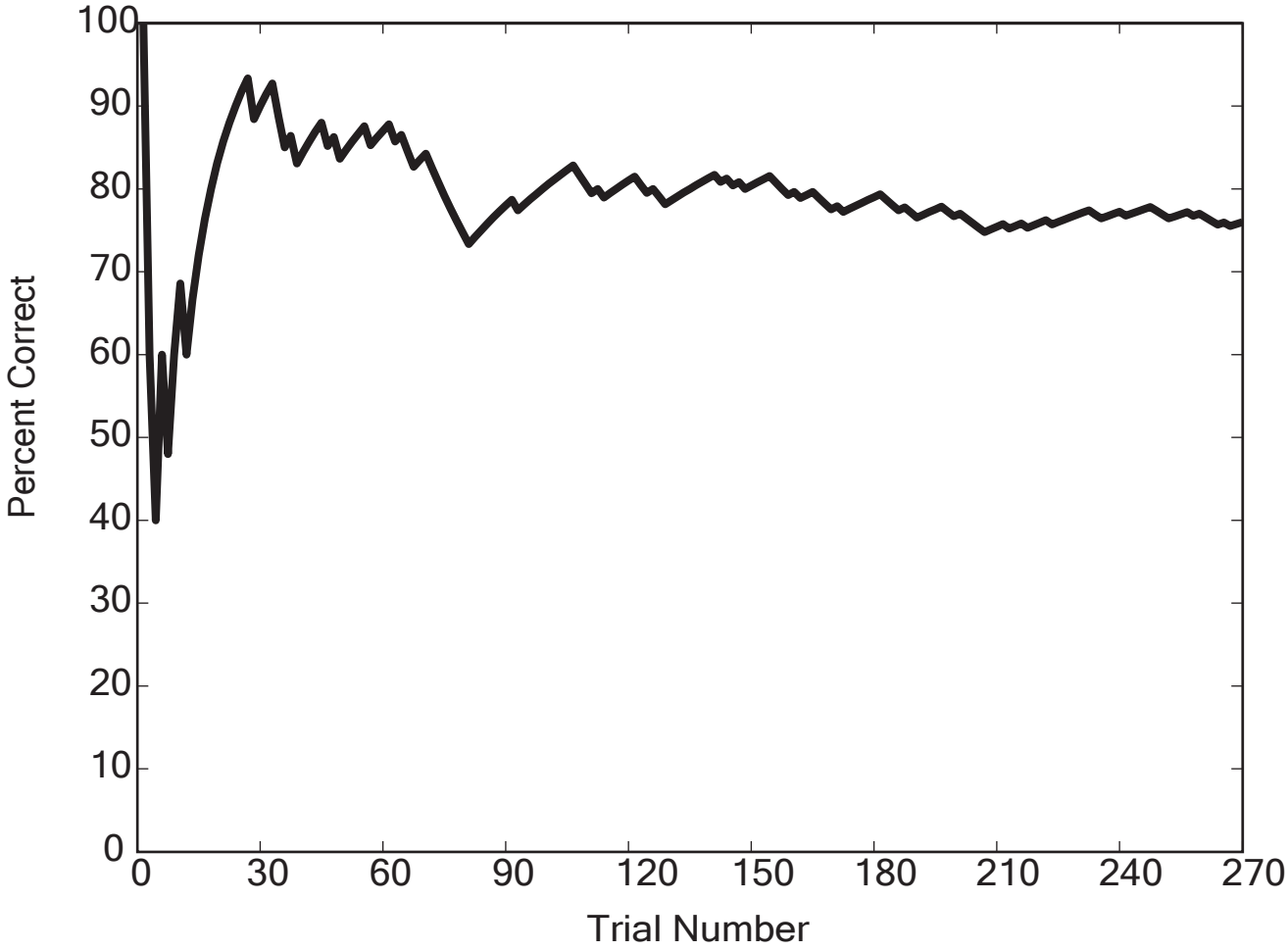
Percent Correct
100
90
80
70
60
50
40
30
20
10
0
0
30
60
90
120
150
180
210
240
270
Trial Number

Figure S2

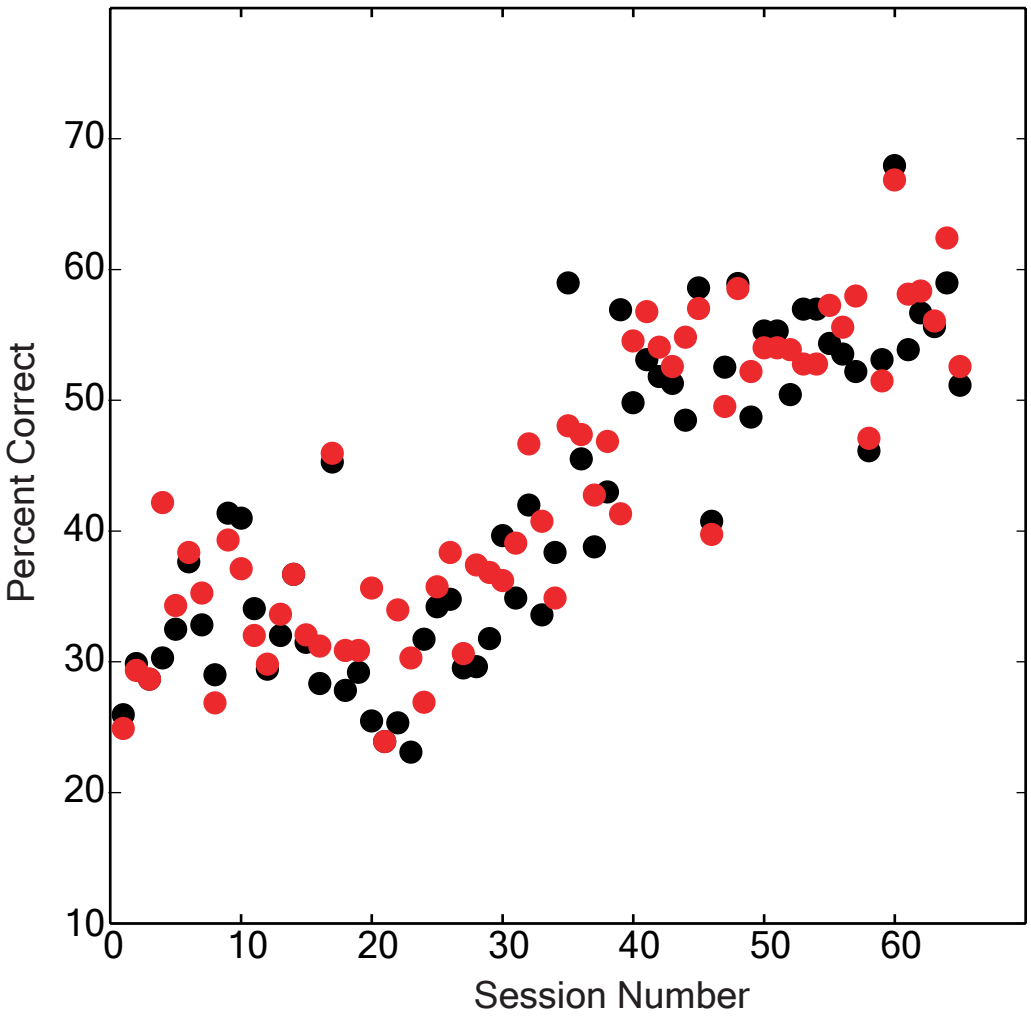
Percent Correct
Session Number
10
20
30
40
50
60
70
0
10
20
30
40
50
60

Figure S3

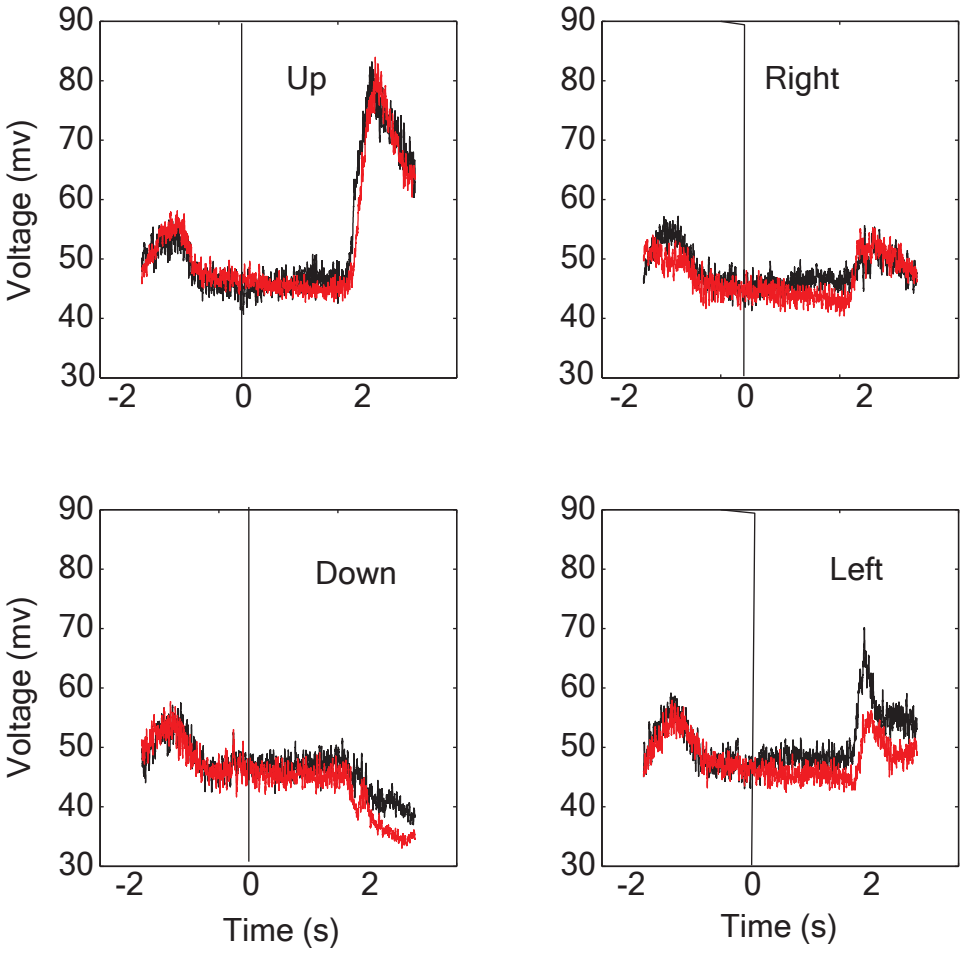
Up
Right
Down
Left
Voltage (mv)
Voltage (mv)
Time (s)
Time (s)
90
80
70
60
50
40
30
-2
0
2

Figure S4

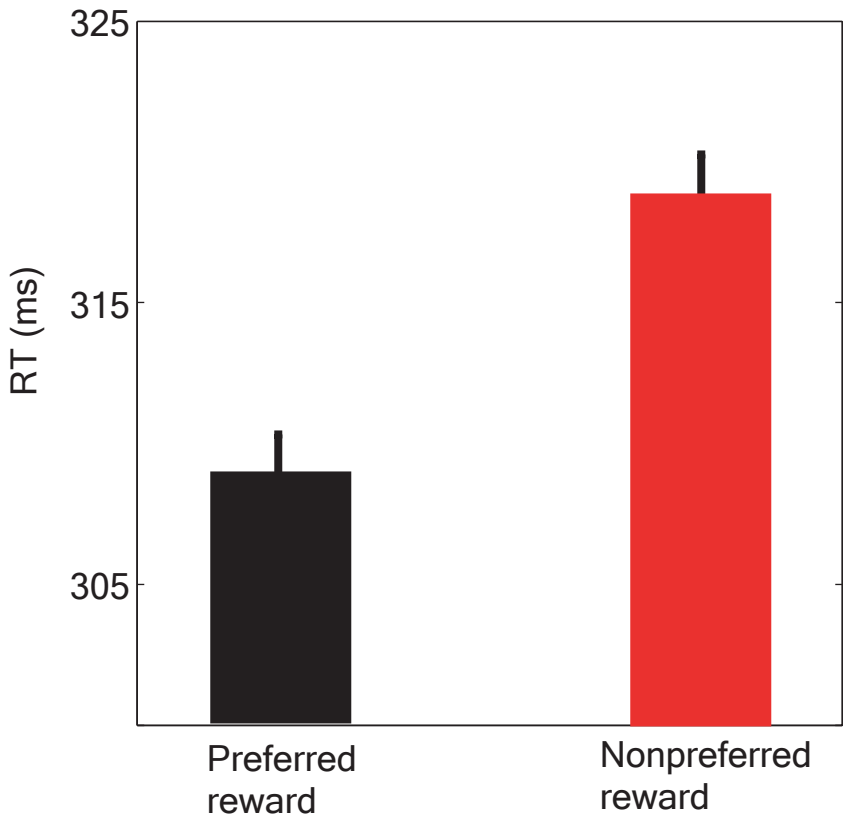

Figure S5

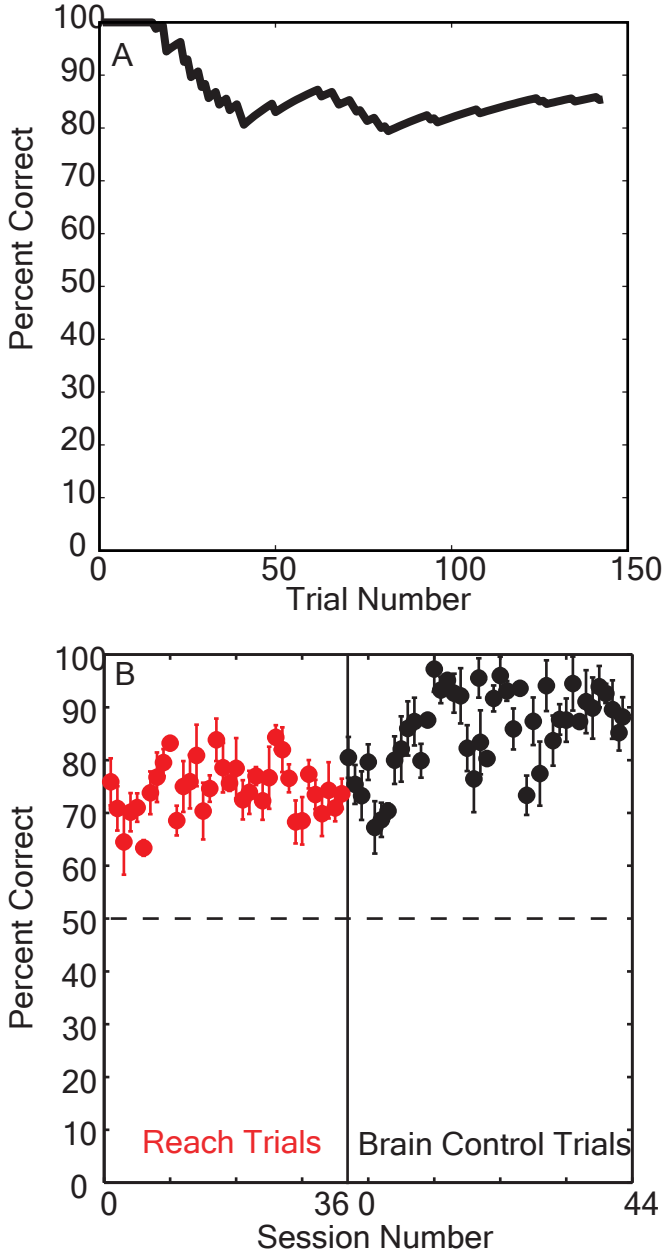
A
Percent Correct
Trial Number
B
Reach Trials
Brain Control Trials
Session Number

Figure S6

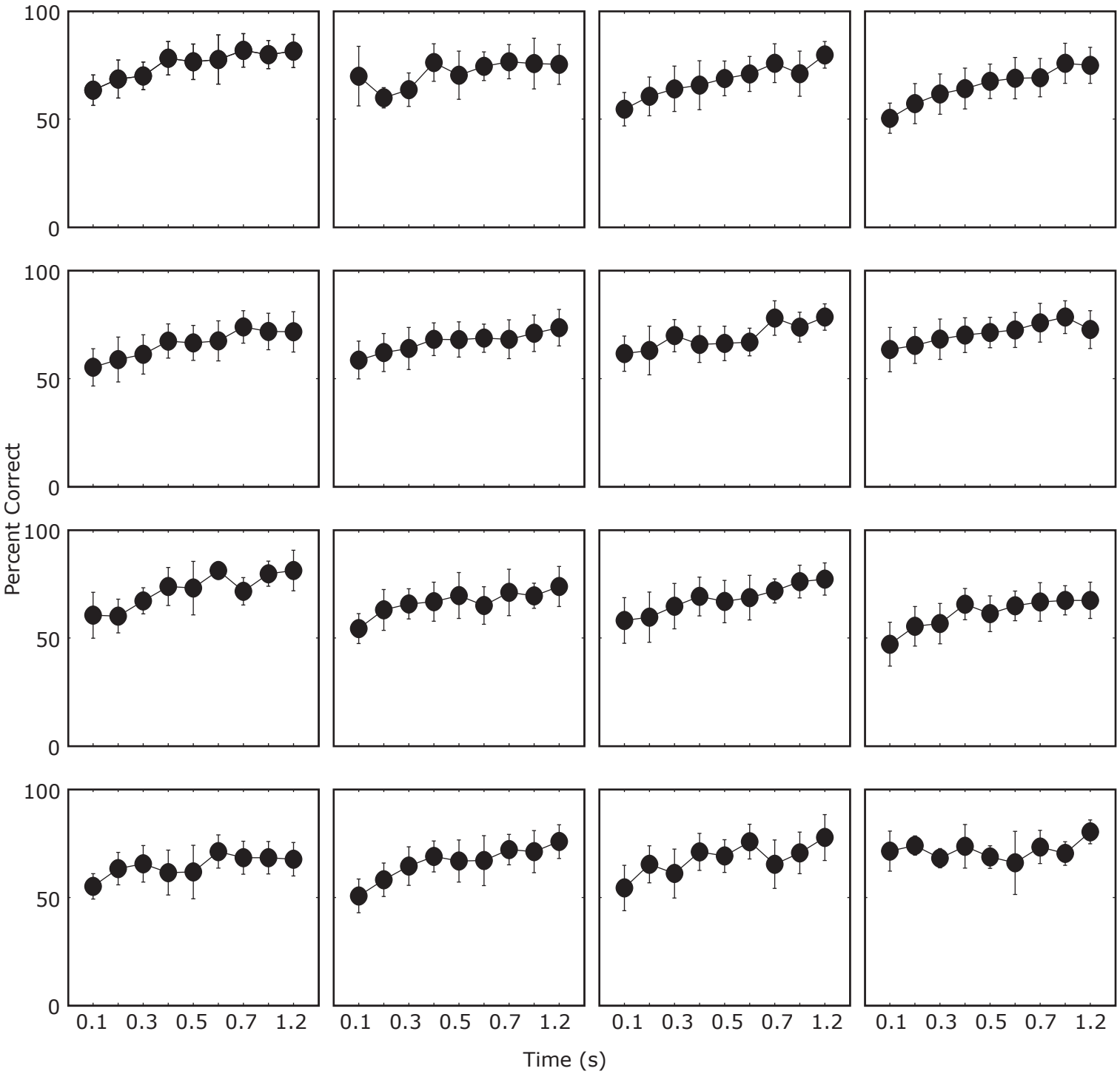

References

1. H. Scherberger *et al.*, *J Neurosci Methods* **130**, 1 (2003).
2. S. Cao, PhD Thesis. *Department of Electrical Engineering* (2003).
3. S. Mallat, *A Wavelet Tour of Signal Processing* (Academic Press, 2001).
4. A. Grunewald, J. F. Linden, R. A. Andersen, *J Neurophysiol* **82**, 330 (1999).
5. S. P. Strong, R. Koberle, R. R. D. van Steveninck, W. Bialek, *Phys Rev Let* **80**, 197 (1998).
6. T. M. Cover, J. A. Thomas, *Elements of Information Theory* (John Wiley and Sons, 1991).